

PYRITE MINE WASTES HYPERSPECTRAL MONITORING AS A TOOL TO DETECT CLIMATE CHANGE

A. Rianza^a, C. Ong^b, A. Müller^c

^a Geological Survey of Spain (IGME), Tres Cantos (Madrid, Spain)

^b CSIRO Exploration and Mining, Kensington, Australia

^c DLR_ German Aerospace Research Establishment, Remote Sensing Data Centre, Oberpfaffenhofen, Deutschland
a.riaza @igme.es

Commission VII, WG VII/1

KEY WORDS: hyperspectral sensors, geoindicators, climate change, mine waste, water quality.

ABSTRACT:

Monitoring of mine waste on sulphide deposits through remote sensing hyperspectral data contributes to predict surface water quality estimating quantitatively acid drainage and metal contamination on a yearly basis. The mineralogy of the surface crusts loaded with highly soluble salts is a record of available humidity and temperature along the year. A temporal monitoring of salt efflorescence on mine wastes at a mine site in the Iberian Pyrite Belt (Spain) has been mapped in this work using hyperspectral airborne Hymap data. Climate change estimations are made based on oxidation stages derived from well-known sequences of minerals tracing sulphide oxidation intensity, using archive spectral libraries. Therefore, mine waste weathering products of sulphide mapped from remote sensing airborne hyperspectral data can be used as a short-term record of climate change, providing a useful tool to assess environmental Geoindicators in semi-arid areas.

1. 1. INTRODUCTION

Rapid oxidation and evaporation of sulphides on mine waste produces iron-bearing sulphate and other metals as secondary minerals. Temperature and humidity control evaporation. On regions with a semi-arid climate where the water table is low and there is a yearly rainy and dry season, sulphate salts growth reaches a maximum at the end of the dry season. Then, the mineralogy of the precipitated salts is a record of available humidity and temperature along the year.

Climate is the controlling factor on the growth and solution of salts from pyrite and other metallic sulphide on mine waste. Most of the previous work mine waste mapping with hyperspectral data is addressed to produce environmental evidence predicting metal contamination concentration and acid drainage both on surface water and groundwater. With this study, we are using the same method and principles to estimate changes on environmental moisture availability and evaporation rate.

Geoindicators are high-resolution measures of short-term changes in the geological environment, which are significant for environmental monitoring and assessment (Berger and Iams, 1996). Most use of remote sensing as an environmental monitoring method emphasizes on broad scale imagery (Laval, 1986). The work that is described below summarizes on a single tracing technique, the surface processes typical of semi-arid environment on mine waste witnessing climate, assessing both surface water and groundwater quality in an annual time frame. It also provides traceable records of climate change using small scale targets and high spatial and spectral resolution imagery, able to provide records of climate effects.

1.1 Hyperspectral studies on Mine Waste

High spectral resolution on airborne and satellite spectrophotometers has enlarged the mapping capabilities of

remote sensing data, developing widely with the use of AVIRIS data operating since 1988. Advances on data calibration and the development of algorithms able to extract information from a large number of spatial spectral data based on field spectra, encouraged applications on environmental issues. Early focus on mine wastes through the study of secondary minerals began concentrating initially on iron-bearing oxides and hydroxides (Farrand and Harsanyi, 1995). It expanded soon to secondary minerals related to mine waste weathering (Clark et al, 1998; Swayze et al, 1996; Levesque, 1997). Minerals generating acid environments attracted the attention of the geological scientific community since they are highly mobile on the environment through solution on drainage water. The spectral behaviour of pyrite and sulphate derived by oxidation, and their solution properties was explored, and patterns of precipitation established and traced using remote sensing hyperspectral data (Swayze et al, 1998; 2000). The development of spectral libraries from field sites has favoured the nearly automatic mapping of ephemeral mineral features related to acid mine drainage (Ong et al, 2002; Montero et al, 2002; Ong et al, 2003; Mars and Crowley, 2003; Sares et al, 2003).

1.2 Regional Geology and Climate

Pyrite mining on the Iberian Pyrite Belt (Southwest Spain and Portugal) extends through history along 5000 years at least (Leblanc et al, 2000). Massive sulphide deposits hosted on a Volcano-sedimentary Complex, a thick stratigraphical series of volcanic detrital origin, are widespread throughout the region (Almodovar, 1998). This geological frame provides high geoavailability for pyrite oxidation. The water quality on the rivers flowing through the area is subject to seasonal variations related to rainfall rate (Olias, 2004).

The mine site of study is located on the inner mountain chain with low altitude near the Atlantic coast (fig. 1). The regional climate follows a Mediterranean climate trend smoothed by the

influence of the Atlantic Ocean (Font Tullot, 1983). The Mediterranean climate is characterized by a wet season from October through May, and a dry season from late May through the summer. The insolation rate is extremely high throughout the year. Low precipitation rate defines a semi-arid climate with permanently low water table. Industrial operation on most metallic mine sites in the Iberian Pyrite Belt is stopped today. Most mine facilities are abandoned and under environmental control of the authorities. They are numerous and the wide regional exposure of abandoned mine waste makes the Iberian Pyrite Belt a training field to test environmental monitoring methods.

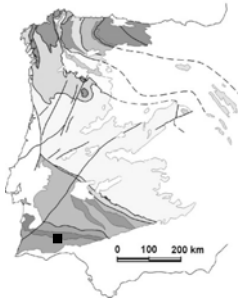


Figure 1. Location of the area of study in the Iberian Massif (Spain and Portugal).

1.3 Pyrite Mine Waste Weathering

Mine sites of metallic sulphide ore deposits are nowadays in many countries undisturbed by industrial activity, exposed to the atmospheric agents. Pyrite, the iron disulphide mineral, is then prone to oxidation under rates only controlled by atmospheric conditions. Pyrite oxidation is a complex process that proceeds rapidly when this mineral and other sulphides are exposed to air, releasing sulphate into water and lowering water pH values (Nordstrom and Alpers, 1999).

Soluble secondary salts are formed from the evaporation of acid-drainage waters. Efflorescent crusts are common on the surfaces and on the edges of natural and mine-drainage streams and ponds. The mineralogy of the product salt can change with progressive evaporation of acid water (Nordstrom and Alpers, 1999). The greatest salt growth occurs when the growing crusts are replenished by acid water, such as a flowing drainage stream or waters wicked to the surface of mine waste dumps by capillary action (Plumlee, 1999). The soluble secondary salts can also form as weathering products of sulphide that are in contact with atmospheric moisture.

Due to their high solubilities, secondary salts form where sulphides have been exposed to weathering by oxygenated waters. Mine waste piles, mine workings and mill tailings are hosts for these minerals.

Particles in finely milled ore and tailings have very high surface areas and abundant broken crystal edges. This enhances mineral reactivity relative to those of mined rock and waste rock (Plumlee, 1999). Oxidation rates on sulphide mine-waste dumps are six orders of magnitude high than granite piles. The reaction of pyrite oxidation is highly exothermic, increasing the environmental temperature around mine waste significantly.

Climate plays an important role in the development of salt crusts on mine waste dumps of abandoned ore bodies to oxidation (Seals and Hammarstrom, 2003). Temperature and humidity are the prime variables that control evaporation. Arid environments are prone to concentrate metals and acidity potential because of the concentrating effects of the evaporation

of mine effluent and the resulting storage in highly soluble metal-sulphate salt minerals. Low water tables in semi-arid climate increase the exposure of waste to air, favouring deep weathering and sulphide oxidation profiles (Plumlee, 1999).

At the end of the rainy season, mine dumps and mud tailings are relatively saturated with water and afterwards begin to dry progressively. As they dry up and ventilate, sulphide oxides to sulphate, the pH falls and the pollutants solubilize. The concentration of water-soluble sulphate and heavy metals increases with declining moisture. These solubilized elements, with evaporation, rise by capillary action to the surface, forming a white salty crust composed of Fe^{2+} and other metals hydrated sulphates.

A sequence of salts from early to later formed is established from a solution of pyrite (Buurman, 1975; Alpers et al, 2003). Ferrous sulphate salts are found close to pyrite sources (melanterite $Fe^{2+}(SO_4) \cdot 7(H_2O)$, rozenite $Fe^{2+}(SO_4) \cdot 4(H_2O)$, szomolnokite $Fe(SO_4) \cdot H_2O$), whereas Ferric-bearing minerals (rhomboclase $HFe^{3+}(SO_4) \cdot 2 \cdot 4(H_2O)$, voltaite, halotrichite $Fe^{2+}Al_2(SO_4) \cdot 4 \cdot 22(H_2O)$) can be considered hydrologic dead-ends, where most of the Fe^{2+} has had time to oxidize to Fe^{3+} .

Further oxidation leads to the formation of schwertmannite ($Fe_3O_{16}(OH)_{12}(SO_4)_2$) and the group of jarosite-alunite ($(SO_4)_2KFe_3(OH)_6$, $KAl_3(SO_4)_2(OH)_6$). The mineralogy of oxidized zones on gossans is dominated by hematite (Fe_2O_3), goethite ($FeO(OH)$) and jarosite ($(SO_4)_2KFe_3(OH)_6$).

Preliminary work mapping the Sotiel mine site in the Iberian Pyrite Belt using Hymap data orientated to contamination estimations precedes this work (Zabcic et al, 2005).

2. METHOD

2.1 Dataset

Hymap airborne hyperspectral data were collected on 6th May 1999, and 19th May 2004, and on 14th August 2004, and 17th June 2005 over the Sotiel minesite in the Iberian Pyrite Belt (Spain). The spatial resolution fluctuates from 5 m in 1999 to 4 m in 2004 and 2005. Pre-processing was performed with routines developed by Hyvista (Cocks et al, 1998) and the German Space Establishment DLR (Richter and Schläpfer, 2002; Schläpfer and Richter, 2002).

Five years lapse from the first flight (May 1999) to the second flight (May 2004). Both flights record the state of pyrite weathering at the end of the wet season, before the intense evaporation process starts, which should progress during the dry season. The three flights from May 2004 to June 2005 cover one year. The first flight took place at the end of the humid season (May 2004). The state of oxidation at the peak of the dry season the same year is traced by the August 2004 flight. The last flight takes place one year later in the middle of an extremely dry and warm summer (June 2005).

Rainfall and temperature records from the weather station of Ronda (Instituto Meteorológico Nacional, Huelva), are considered from 1998 to 2005 (fig.2). The hydrological year begins typically with an intense rain event in October, and minor rainfall along autumn and spring. The very dry and warm season starts in May and reaches minimum rainfall in August. The temperature estimations respond to a complex evaluation of weather and climate parameters (Instituto Meteorológico Nacional, www.inm.es).

The autumn 1998 was normal temperature and very dry, followed by a normal temperature and very dry winter 1999. The spring 1999 was dry and warm. Water availability was scarce in May 1999, and relatively mild temperatures would

indicate low evaporation and possible preservation of soluble salts from the previous year.

Autumn, winter and spring before May 2004 were very humid and warm. The following summer was extremely warm and dry, suggesting high evaporation rates. Intense pyrite oxidation products would grow, which should be present in August 2004. The following year was very dry and warm. Water availability was scarce, and further evaporation would strengthen oxidation. The June 2005 flight should summarize the results through mine waste weathering products.

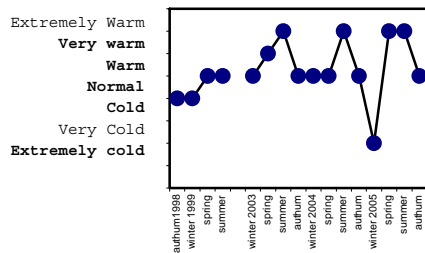


Figure 2. Temperature records during the time span previous to the analysed imagery (Ronda station, Instituto Meteorológico Nacional, Spain, www.inm.es).

Fieldwork was conducted in summer 2005 and 2006. Samples were collected over the mine waste dumps and the Odiel river flow path and sides. Field spectra were collected using an ASD Fieldspec-pro Spectrophotometer both for calibration and interpretation purposes. Laboratory spectral measurements on those samples were taken with a Perkin Elmer Lambda 9 Spectrophotometer provided with an integrating sphere, in the visible and near infrared wavelength range (0.4 μm -2.4 μm) with a spectral resolution of 0.001 μm . Samples both from loose material and crusts formed over the ground on mine dumps and river sediments, were measured to ascertain spectral differences related to dehydration, oxidation and subsequent compaction from solutions after rainy events. Selected samples of crusts and loose material from the mine dump were analysed by X-ray diffraction.

2.2 Image processing

Hyperspectral imagery provides wide possibilities to map complex features of the surface of the earth, offering a high dimensionality of data, if careful signal to noise ratio and good spatial resolution are ensured. The procedure for feature extraction for thematic purposes used on this work is an interpreter oriented sequential spectral unmixing using standard algorithms, leading to a spatial pattern and spectral identification on the scene (Hubbard and Crowley, 2005) summarized on a map. The dimension of the data is reduced along various image processing steps tailored to the scene, ending on a map of pyrite oxidation products on the abandoned mine site.

The first step uses a false colour composite with Hymap channels 10, 39 and 125 to build a spectral library with basic land use end-members on the scene. Spectral Angle Mapper produces a first estimation of the spectral diversity of open land, which is digitally used as a mask on subsequent image processing steps. Areas mainly covered by vegetation, clear water and urban areas are excluded for analysis from this step on.

The areas mapped as open land on the first step are explored by Minimum Noise Fraction transforms, subsequent Pixel Purity

Index (Boardman, 1993) and n-dimensional analysis. Mine sites and the main areas covered by sulphate salts are commonly identified from bare open and cultivated land at this stage. The data dimensions are reduced further, repeating the procedure to qualify areas within early-formed salts and among the more oxidized zones, which are isolated on corresponding masks. A final map is compiled gathering all endmembers corresponding to pyrite oxidation products on the scene. A spectral library is finally built with such endmembers, which are then mineralogically identified using a selection from archive spectral libraries.

Spectral Angle Mapper (Kruse, 1993) is used to test scene similarity from the second step, helping to identify endmembers more representative of sulphate salt coverage according to field experience and comparison with the shape of the corresponding spectra with archive spectral libraries. Spectral shape information is so derived from Hymap data.

A number of individual mineral substances precipitated from pyrite acid water were identified on public domain spectral libraries, ranging from melanterite, the first-formed sulphate, to hematite when dehydration and oxidation is completed (fig.3). Eighteen existing spectra from sulphide oxidation products in public domain spectral libraries (Clark et al, 1993; Crowley et al, 2003) were used as references with the Spectral Analyst (RSI, 2000) to get a comparative score of similarity for spectra from every map unit. Spectral Angle Mapper, Spectral Feature Fitting and Binary Encoding were taken into account on equal weights on the final similarity score. The dominant mineral was assigned to the map units (fig.3).

Comparison with the selected sulphate and iron oxides and hydroxides spectral library through the Spectral Analyst (RSI, 2000) confirms field expectations and prior mineralogical studies. Spectra with dominant hematite, jarosite or alunite can be identified on well-developed areas.

3. SPATIAL PATTERN ON PYRITE OXIDATION PRODUCTS: A CLIMATE CHANGE RECORD

The mine works in Sotiel spread along the river Odiel. The mines on the Iberian Pyrite Belt were already operated by Tartesians and Phoenicians before Roman times. Mining was continuous along the Middle Ages using handcraft methods, up to the intensive operation during the Industrial Revolution in the 19th Century. Today, massive sulphide deposits hosted on basalts were mined until the eighties, when mining stopped. From 1991 to 2001, the ore processing plant of the Sotiel minesite toasted industrial sulphide waste to produce sulphuric acid delivered to the nearby coastal industrial facilities.

The operating underground mine works are displayed along the river Odiel (fig.3). A tape transported the ore from the mine uphill to the ore processing plant. Mill tailings from the ore processing plant are stored on an adjacent dam, which drains to a southerner dam flowing to the river Odiel, upstream from the mine works. The sides of the river show products from precipitations from acid water along the whole length of the flow path.

The observed oxidation patterns shown by hyperspectral image processing on the four Hymap flights are diverse within the mine site. They would be described separately for different domains: the area around the ore processing plant including the two mill tailings dams, the mine works by the river, and the flow path of the river.

3.1 The mine dumps by the river

The mine waste piles at the mine operating works by the river and the riversides are more reliably translating climate effects. In May 1999, copiapite, halotrichite, and partly rozenite are restricted to pools of standing water left by poor water flow (fig. 3). Alunite and jarosite cover the slopes of waste piles, whereas schwertmannite and minor hematite patches occur on the flat top of piles.

The mine waste piles and works by the river, show in May 2004 the schwertmannite flat tops of piles in 1999 oxidized partially to hematite or jarosite; copiapite and halotrichite from ponds oxidize to alunite and jarosite; jarosite slopes oxidize to goethite. The general trend from May 1999 to May 2004 is clearly increasing oxidation.

The dry period from May to August 2004 increases dehydration and oxidation. The waste flat tops are homogeneously covered by hematite; goethite is generalized on slopes, and the extent of schwertmannite is reduced.

The same emphasized oxidation trend is displayed in June 2005 on the waste at the riverside mine works in comparison with August 2004, after an extremely dry and warm year. Hematite is homogeneously consistent on flat tops of piles, goethite, jarosite and alunite grow on the slopes, and halotrichite spreads on shallow ponds among the waste piles.

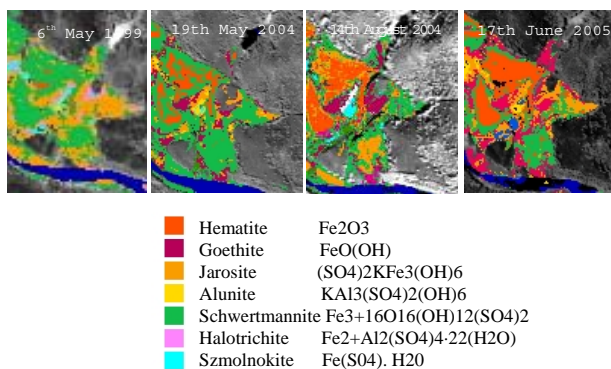


Figure 3. Maps compiled from Hymap data on the minerals product of oxidation and dehydration of sulphide waste, arranged on a precipitation and oxidation sequence. Detail of the mine dump by the river.

3.2 The river flow path

Sulphate salts and pyrite oxidation products border the bottom, banks and sides of the river Odiel, of varying mineralogy and height depending on flow rate and climate. The oxidation products grow over river sediments or underlying rock, and their occurrence is independent from industrial operation or mine works. Jarosite and schwertmannite are the most frequent salts. Jarosite tends to develop over the boulders and sands of the riverbanks (fig. 4). Schwertmannite grows on a ribbon along the steeper sides of the flow path. Melanterite may appear on isolated pools, preferably on severe drought times, when flow rate lessens.

The extent of jarosite shrinks from May 1999 to May 2004. The very humid time up to the spring 2004 is responsible for the reduction on oxidation products. The surface covered by jarosite expands during the summer, and spots of goethite point up on steeper sides in August 2004.

The picture of the river in June 2005, after a whole year of drought and warm temperature, is dramatically oxidized. Most schwertmannite has oxidized to goethite and alunite. Melanterite and rozenite are occasionally present on small pools of standing water on the bottom of the river. Jarosite remains only on the upper sandbanks. Schwertmannite shows a preference for gentle slopes, whereas goethite occurs on steep surfaces which are quickly abandoned by water for the season. Complete absence of flooding water on the flow path permits a deeper oxidation within the period of drought.

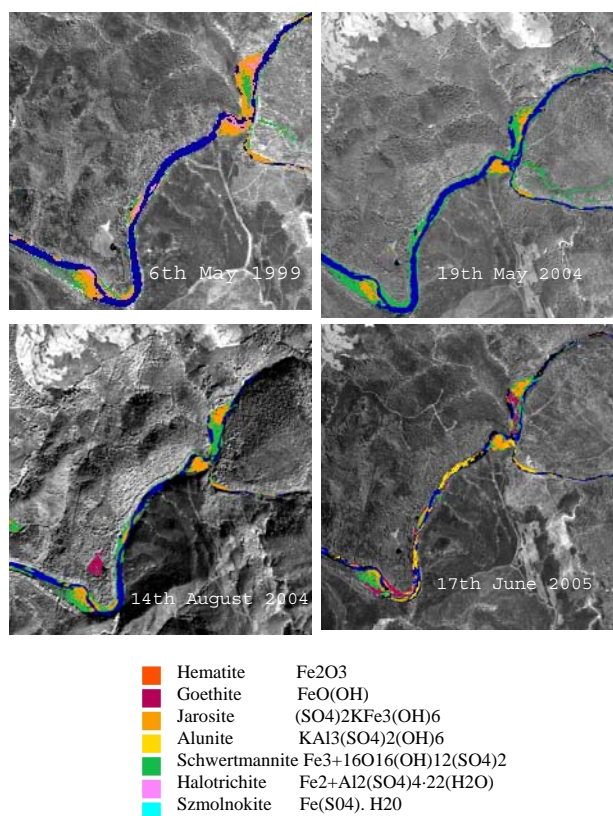


Figure 4. Maps compiled from Hymap data on the minerals product of oxidation and dehydration of sulphide waste, arranged on a precipitation and oxidation sequence. Detail of the river flow path.

3.3 Field and laboratory spectra

Spectral measurements were made in the field with an ASD Spectrometer. Also, samples were collected in the field from representative geological targets and measurements were made in the laboratory with a Perkin Elmer Lambda Spectrometer (fig.5). Mineral growth during pyrite oxidation results on a heterogeneous spatial pattern. However, mineralogically homogeneous areas can be recognized on the imagery with a strong geomorphological control. Flat areas, and slopes, host the areas where the mineralogical evolution can be traced. Hymap spectral responses from the mapped regions of interest are particularly reliable on both oxidation or hydrated ends on the mineral sequence (hematite and halotrichite or szmolnokite on our test site). Both mine dumps and river sediments or flow path display less mineralogical variability than pyrite mud.

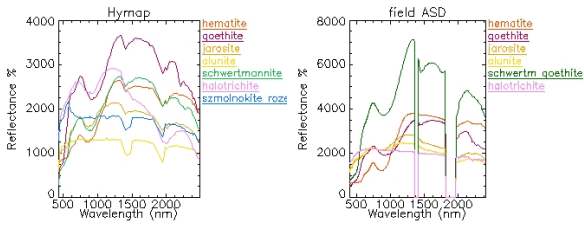


Figure 5. Spectra from Hymap mapped areas and field taken with an ASD spectrometer

4. DISCUSSION

Iron sulphide weathers rapidly producing a sequence of sulphate salts, which are also highly soluble. The ore processing plant of the mine facility was still operating at the beginning of the study. Tailings would be released to the dams, changing the composition and evolution of both the surrounding areas and the previously stored mud tailings. Even after the ore processing plant stopped its activity, the site was environmentally controlled, and a water cleaning plant at the foot of the southern tailings dam was active. The interpretation of the mineral composition of crusts growing in the area in terms of climate change has to take into account the active industrial influence.

The oxidation pattern on the mine site is clearly established using archive spectral library references to map airborne hyperspectral Hymap data. A progressive oxidation is observed with increasing temperatures from spring 2004 to summer 2005. The path of growth of individual minerals on a certain surface can be followed confirming or discrediting the general trend. This is also true for weathering products growing on riversides along river courses with acid drainage water.

The oxidation patterns follow different trends on mud tailings than on waste piles. Fine particles in mud tailings favour mineral reactivity (Plumlee, 1999). In addition, mud tailings is a homogeneous viscous mass with a smooth outer surface sheltering rainwater, which dissolves the upper weathering products rapidly. Mud tailings are witnesses of short weather events. Mine waste piles are more resistant to weathering because of their coarse particles. They respond to weather events slower than mud tailings, acting as more reliable traces of seasonal or longer periods of climate change.

The maps compiled using hyperspectral analysis of Hymap data describe faithfully the diverse weathering trend of mud tailings and mine waste piles. Mine waste piles on completely abandoned mine sites and riversides of acid mine drainage flowing water are preferred to record effects of climate change on a long term basis. For that purpose, hyperspectral remote sensing data must be taken at chosen dates related to the weathering seasonal evolution dependent on humidity and temperature.

To produce maps that can describe this very detailed evolution, hyperspectral image processing has to be applied sequentially identifying the areas critical on the mine site, and related to mine site weathering products, such as riversides. The image processing procedure must be applied to subscenes isolating the target areas. Different image processing procedures can be necessary per subscene to reach a map responding to the maximum spectral complexity of the target, in terms of weathering products.

5. CONCLUSIONS

Sulphide mine waste in semi-arid environment can be used as a small scale target to provide information of short-term climate changes. Therefore, it may be included among Geoindicators, when hyperspectral remote sensing is used as a monitoring tool. Hyperspectral data have been able to distinguish different degrees of oxidation and dehydration on pyrite mud tailings and waste piles on an abandoned mine facility. Mineral indicators of such stages are suggested using the spectral analysis techniques comparing with spectral libraries collected from foreign samples to the study site.

The salt sequence on the oxidation process is confirmed on the most stable areas on the mine facility. The annual monitoring of weathering products at the end of the wet season and the climax of the dry season, can be used as a climate record. Changes on evaporation, humidity and temperature can be inferred from the mine waste weathering product maps.

Effect of particle size on the evaporation mineralogical pattern is critical on mineral reactivity. Mill tailings both around the ore processing plant and both dams display fresh weathered products of pyrite more easily. Mine waste dump piles and salts precipitated along the flow path of flowing acid water are more reliable to display seasonal climate effects, independent of sparse rain events or water transfer during mine waste operation actions.

Image processing must be tailored per scene and per domain within the mine site. Otherwise, the spatial mineralogical pattern is lost, as well as the interpretation ability in terms of climate change, and metal contamination estimations or acid drainage prediction. The resulting maps agree on their conclusions when applying separately image processing to subscenes, but they would never be shown through a unique image processing sequence applied to the whole scene.

6. REFERENCES

- Almodovar, R., Saez, R., Pons, J.M. and Maestre, A., 1998. Geology and genesis of the Aznalcóllar massive sulphide deposits, Iberian Pyrite Belt, Spain. *Mineralium Deposita* ,33, pp.111–136.
- Alpers, C.N., Nordstrom, D.K., and Spitzley, J., 2003, Extreme acid mine drainage from a pyritic massive sulfide deposit: the Iron Mountain endmember. In Jambor J.L. and Blowes D.W. and Ritchie, A.I.M. (Eds.), *Environmental Aspects of Mine-Wastes*, pp. 407-430. Ottawa: Mineralogical Association of Canada.
- Berger, A.R. and Iams W.J., 1996. *Geoindicators: Assessing rapid environmental changes in earth systems*. Rotterdam: A.A. Balkema.
- Boardman, J. W., 1993. Automated spectral unmixing of AVIRIS data using convex geometry concepts. In *Summaries Fourth JPL Airborne Geoscience Workshop*, (Washington, D.C.), JPL Publication pp. 93-26, 1, 11 - 14.
- Buurman, P., 1975. In vitro weathering products of pyrite. *Geologie Mijnbouw*, 54, pp. 101-105.
- Clark, R.N., Swayze, G.A., Gallagher, A., King, T.V.V. and Calvin, W.M., 1993), The U.S. Geological Survey Digital Spectral Library: Version 1: 0.2 to 3.0 mm. *U.S. Geological Survey, Open File Report* pp. 93-5 92.
- Clark, R.N., Vance, J.S. and Livo, K.E., 1998. Mineral Mapping With Imaging Spectroscopy: The Ray Mine, Az, From: Mineral Mapping with Imaging Spectroscopy: the Ray Mine, AZ. Roger N. Clark, Sam Vance, Rob Green, *Summaries of the 7th Annual JPL Airborne Earth Science Workshop*, R.O. Green, Ed., JPL Publication 97-21. Jan 12-14, pp. 67-75.

- Cocks, T., Jossen, R., Stewart, A., Wilson, I. and Shields, T., 1998. The HymapTM Airborne Hyperspectral Sensor: The system, calibration and performance. *Proceedings 1st EARSEL Workshop on Imaging Spectroscopy*, Zurich, October 1998, pp. 37-42.
- Crowley, J.K., Williams, D.E., Hammarstrom, J.M., Piatak, N., Chou, I-M. and Mars, J.C., 2003. Spectral reflectance properties (0.4–2.5 μm) of secondary Fe-oxide, Fe-hydroxide, and Fe-sulphate-hydrate minerals associated with sulphide-bearing mine wastes. *Geochemistry: Exploration, Environment, Analysis*, 3- 3, pp. 219-228(10).
- Farrand, W.H. and Harsanyi, J.C. 1995. Mineralogic Variations in Fluvial Sediments Contaminated by Mine Tailings as Determined From AVIRIS Data, Coeur d'Aldene River, Idaho. *AVIRIS Workshop*, pp. 47-50, JPL Publication.
- Font Tullot, I., 1983): *Climatología de España y Portugal*. Madrid, 296 p. Madrid: Instituto Nacional de Meteorología Publications.
- Hubbard, B.E. and Crowley, J.K., 2005. Mineral mapping on the Chilean-Bolivian Altiplano using co-orbital ALI, ASTER and Hyperion imagery, Data dimensionality issues and solutions. *Remote Sensing of Environment*, 99, pp. 173-186. Instituto Nacional de Meteorología, Spain, *Resumen Anual Climatológico de los años 2003, 2004 y 2005*. www.inm.es
- Kruse, F.A., Lefkoff, A.B., Boardman, J.B., Heidebrecht, K.B., Shapiro, A.T., Barloon, P.J., and Goetz, A.F.H., 1993). The Spectral Imaging Processing System (SIPS) – Interactive Visualization and Analysis of Imaging Spectrometer Data. *Remote Sensing of Environment*, 44, pp. 145-163.
- Laval, K. 1986. General circulation model experiments with surface albedo changes. *Climatic Change*, 9, 1-2, pp. 91-102.
- Leblanc, M., Morales, J.A., Borrego, J. and Elbaz-Poulichet, 2000. A 4500 years old mining pollution in Southwestern Spain: Long-Term concerns for modern mining. *Economic Geology*, 95, pp. 655-672.
- Lévesque, J., Szeredi, T., Staenz, K., Singhroy, V. and Bolton, D., 1997. Spectral Unmixing for Monitoring Mine Tailings Site Rehabilitation, Copper Cliff Mine, Sudbury, Ontario. *Twelfth International Conference and Workshops on Applied Geologic Remote Sensing*, Denver, Colorado, 17-19 November 1997, pp. 340-347.
- Mars, J.C. and Crowley, J.K., 2003. Mapping mine wastes and analyzing areas affected by selenium-rich water runoff in southeast Idaho using AVIRIS imagery and digital elevation data. *Remote Sensing of Environment*, 84, 3, pp. 422-436.
- Montero, I. and Brimhall, G., 2002. Multiplatform VIS/SWIR Hyperspectral Approach to the Study of Acid Mine Drainage from Abandoned Mines. *Denver Annual Meeting Geological Society of America* 2002, 43507.
- Nordstrom, D.K. and Alpers, C.N., 1999. Geochemistry of acid mine waters. In Plumlee G.S. and Logsdon M.J.: The Environmental Geochemistry of Mineral Deposits. Part A: Processes, Techniques, and Health Issues. *Reviews in Economic Geology*, 6A, pp. 133-160.
- Ong, C. and Cudahy, T., 2002. Deriving Quantitative Monitoring Data Related to Acid Drainage Using Multi-temporal Hyperspectral Data. *AVIRIS Workshop*, 5pp.
- Ong, C., Cudahy, T.J. and Swayze, G., 2003. Predicting Acid Drainage Related Physicochemical Measurements Using Hyperspectral Data. *Proc. 3rd EARSEL Workshop on Imaging Spectroscopy*, Herrsching, 13th-16th May 2003, pp. 363-369.
- Olias, M., Nieto, J.M., Sarmiento, A.M., Cerón, J.C. and Canovas, C.R., 2004. Seasonal water quality variations in a river affected by acid mine drainage: the Odiel River (South West Spain). *Science of The Total Environment*, 333, 1-3, pp. 267-281.
- Plumlee, G.S., 1999. The environmental geology of mineral deposits. Part A: Processes, Techniques, and Health Issues. *Reviews in Economic Geology*, 6A, pp. 71-116.
- Richter, R. and Schläpfer, D., 2002. Geo-atmospheric processing of airborne imaging spectrometry data. Part 2: atmospheric/topographic correction, *International Journal of Remote Sensing*, 23, pp. 2631-2649.
- RSI, 2000. ENVI User's Guide, Research Systems Inc. Publications.
- Sares, A., Hauff, Ph.L., Peters, D.C., Coulter, D.W., Bird, D.A., Henderson III, F.B. and Prosh, E.C., 2003. Characterizing Sources of Acid Rock Drainage and Resulting Water Quality Impacts Using Hyperspectral Remote Sensing – Examples from the Upper Arkansas River Basin, Colorado. *Proceedings Geospatial Conference*, December 7th-9th 2004, Atlanta (GA, USA), pp 20.
- Schläpfer, D. and Richter, R., 2002. Geo-atmospheric processing of airborne imaging spectrometry data. Part 1: parametric orthorectification. *International Journal of Remote Sensing* 23, pp. 2609-2630.
- Seals II, R.R. and Hammarstrom, J.M., 2003. Geoenvironmental models of mineral deposits: examples from massive sulfide and gold deposits. In Jambor, J.L. Blowes, D.W. and Ritchie, A.I.M. (2003), *Environmental Aspects of Mine-Wastes*, pp. 11-51. Ottawa: Mineralogical Association of Canada.
- Swayze, G.A., Smith, K.S., Clark, R.N., Sutley, S.J., Pearson, R.M., Vance, J.S., Hageman, Ph.L., Briggs, P.H., Meier, A.L., Singleton, M.J., and Roth, S., 2000. Using imaging spectroscopy to map acidic mine waste. *Environmental Science and Technology*, 34, pp. 47-54.
- Swayze, G.A., Clark, R.N., Smith, K.S., Hageman, P.L., Sutley, S.J., Pearson, R.M., Rust, G.S., Briggs, P.H., Meier, A.L., Singleton, M.J. and Roth, S., 1998. Using Imaging Spectroscopy To Cost-Effectively Locate Acid-Generating Minerals At Mine Sites: An Example From The California Gulch Superfund Site Airborne Visible/Infrared Imaging Spectrometer (AVIRIS): 1998 *JPL Airborne Geoscience Workshop Proceedings*, Leadville, Colorado, 1998, pp. 49-53.
- Swayze, G.A., Clark, R.N., Pearson, R.M. and Livo, K.E., 1996. Mapping Acid-Generating Minerals at the California Gulch Superfund Site in Leadville, Colorado using Imaging Spectroscopy. *Summaries of the Sixth annual JPL Airborne Earth Sciences Workshop*, R.O: Green (ed.), JPL Publication 96-4, March pp. 4-8.
- Zabcic, N., Ong, C., Müller, A., Rivard, B., 2005. Mapping pH from airborne hyperspectral data at the Sotiel-Migollas mine; Calanas, Spain. *Proceedings 4th EARSEL Workshop on Imaging Spectroscopy*, 27th-29th April 2005, Warsaw (Poland), pp. 467-472.

7. ACKNOWLEDGEMENT

Thanks are due to J.M. Moreira and A.Gil for information on mine site inventories belonging to the Servicio de Información y Evaluación Ambiental de Andalucía (Spain). The Instituto Meteorológico Nacional provided historic climate data on the area. The Junta de Andalucía granted entrance to restricted areas of the Sotiel mine site. J.M. Nieto and R. Sáez pointed to critical knowledge on the evolution of weathering minerals of local mine sites. The Science Council of Spain funded part of this work (CGL2005-02462/BTE; CGL2006-01544/CLI).